Multilayered $CaCO_3$/block-copolymer materials via amorphous precursor to crystal transformation

Haofei Gong[a], Manuela Pluntke[b], Othmar Marti[b], Paul Walther[c], Laurie Gower[d], Helmut Cölfen[e], Dirk Volkmer[a]

[a] *Institute of Inorganic Chemistry II, Ulm University, Albert Einstein Allee 11, D-89081 Ulm, Germany*
[b] *Institute of Experimental Physics, Ulm University, Albert Einstein Allee 11, D-89081 Ulm, Germany*
[c] *Central Electron Microscopy Unit, Ulm University, Albert Einstein Allee 11, D-89081 Ulm, Germany*
[d] *Department of Materials Science & Engineering, University of Florida, 210A Rhines Hall, Gainesville, FL 32611, USA*
[e] *Max Planck Institute of Colloids and Interfaces, Colloid Chemistry, Research Campus Golm, Am Mühlenberg, D-14424 Potsdam, Germany*

1. Introduction

Biogenic nacre is well known for its high strength, toughness and hardness [1,2]. Its superior mechanical properties originate from unique structural characteristics: the inner layer of nacre features a highly organized lamellar structure with alternating calcium carbonate (aragonite) and organic matrix layers, which is often referred to as *brick-and-mortar* structure. The calcium carbonate layer has a hierarchical structure consisting of an arrangement of oriented aragonite polygonal tablets with a thickness of some 200–700 nm and lateral dimensions of some 1–5 μm, which include oriented nanograins with lateral dimensions of several tens of a nanometer [3]. These nanograins can deform and rotate under an applied tensile load, which is considered one of the most important reasons for nacre toughness [4]. The organic layer between two adjacent inorganic layers, which is mainly composed of polysaccharides and proteins, also plays a key role for stress distribution and leads to the characteristic toughness, which is suggested to occur through sacrificial bonds [5,6].

These unique material properties of nacre have thus inspired scientists to develop self-organizing composite materials aiming at hierarchical structures with comparably high mechanical performance [7]. For example, Tang et al. [7a] have created nacre-type multilayers by fabricating a Layer-by-Layer electrostatic assembly of clay platelets and polyelectrolytes, which showed mechanical properties similar to nacre. Bonderer et al. [7b] showed that a bottom-up colloid assembly of ceramic platelets and polymer results in hybrid films with high tensile and ductile properties. These studies, however, made use of pre-formed crystalline inorganic building blocks, such as montmorillonite clay [7a] and submicrometer alumina platelets [7b] to obtain layered composite materials. Therefore, the fabrication of artificial nacre containing calcium carbonate and organic matrix layers as yet has remained elusive, owing to the difficulty of producing tabular layers of calcium carbonate crystals through conventional crystallization routes [8,9].

It has been recently proposed that the aragonite tablets from nacre could form via a transient precursor phase of amorphous cal-

cium carbonate (biogenic ACC) [10,11]. Addadi et al. [12] presumed that biogenic aragonite tablets are being formed via a colloidal ACC phase within a silk-like protein gel. Complementary high-resolution TEM studies by Nassif et al. have shown that individual nacre tablets from *Haliotis laevigata* are surrounded by a 3–5 nm thick layer of stable ACC. The authors concluded that there is no direct epitaxial relation between the intercrystalline organic matrix and the nucleating crystal due to the existence of this intervening stable amorphous layer [13].

In light of developing biomimetic mineralization systems leading to nacre-type materials one of our aims is to gain further insights into the putative formation mechanisms of biological nacre. It has been shown that an organic matrix obtained from demineralized biogenic nacre can be filled with calcium carbonate via a polymer-induced liquid precursor (PILP) [9]. Nevertheless, this nacre retrosynthesis approach requires the natural matrix. We here propose a model system which makes use of a PILP phase, [14] which forms beneath a monolayer of a block copolymer of poly(styrene)-*block*-poly(acrylic acid) (PS-*b*-PAA). Block copolymer as a monolayer has been successfully applied as an organic layer to modify the crystallization of calcium phosphate [15]. A polyelectrolyte additive (poly(acrylic acid), PAA) is added to the aqueous subphase solution in order to produce a PILP layer adjacent to the copolymer monolayer, a process which has been successfully applied previously to Langmuir monolayers deposited on glass substrates [16]. Due to its liquid-like properties, the PILP phase of $CaCO_3$ can be molded into various shapes [17]. The subsequent conversion of the PILP layer into a polycrystalline material via a pseudomorphic transformation process thus preserves the particular shape of the PILP and can produce a variety of non-equilibrium crystal morphologies of $CaCO_3$ [18].

Since prior work has shown that an organic/inorganic composite layer could be built on a Langmuir monolayer at the air–liquid interface [16], our second aim is to assemble a nacre-type composite employing a single block-copolymer/PILP layer as a building block. An amphiphilic block copolymer PS-b-PAA was chosen to mimic the intercrystalline organic matrix of nacre since it is known to form a stable monolayer at the air/water interface [19], where it was hypothesized that the hydrophilic polyelectrolyte block would lead to a mechanically strengthened and stable PILP/block-copolymer interface. Moreover, the hydrophobic interactions between PS moieties could provide a means of introducing some elasticity into the composite, which is required to avoid tension when the PILP layer transforms into crystals. In order to form aragonite crystals as an imitation of nacre's aragonite tablet layer, Mg was added into the crystallization solution since it is well known to promote the formation of aragonite crystals [20].

2. Experimental

2.1. Materials

Block copolymer poly(styrene)-*block*-poly(acrylic acid) (PS-*b*-PAA) was purchased from Polymer Source, Inc., with a molecular weight M_w(PS) = 16 000 g/mol and M_w(PAA) = 4300 g/mol. Poly(acrylic acid) (PAA, $M_w \sim 8000$) was purchased from Aldrich. $CaCl_2$, $MgCl_2$, and $NaHCO_3$ were all purchased from Merck. All chemicals were used as received without further purification.

2.2. Procedure

In a typical experiment, an aqueous solution containing 12 mM $CaCl_2$, 12 mM $MgCl_2$ and 6 μg/mL PAA was introduced as subphase into the Langmuir trough. A solution of PS-*b*-PAA (1 mg/mL) in THF/chloroform (1:9) was spread onto this subphase to form a monolayer. After 15 min for solvent evaporation, the monolayer was compressed to a final surface pressure of 20 mN/m. Then the monolayer was kept at constant surface area for 16 h in order to achieve an equilibration of the interactions between subphase and monolayer. After that, an aqueous solution of $NaHCO_3$ (0.7 mol/L, saturated with CO_2 for 2 h) was injected into the subphase of the Langmuir trough. The final concentration of $NaHCO_3$ in the trough was about 0.1 M. After 4 h, a continuous PILP layer formed underneath the monolayer. This film was then transferred horizontally onto solid (glass) substrates by approaching the substrates, both from air and from the subphase, and then lifting them off manually. Multilayers were prepared through repeated Layer-by-Layer transfer of single layers onto glass substrates. The composite single or multilayer was annealed at 150 °C for 4 h leading to PILP-to-crystal transformation.

2.3. Characterizations

Polarized optical microscope studies were performed with an Olympus BX51 microscope. AFM was carried out with an Agilent 5500 instrument equipped with Olympus cantilevers OMCC-AC160TS. The Cryo-SEM sample was prepared by transferring a composite film onto a flat sapphire substrate and then quickly freezing it in liquid propane. The sample was observed with a Hitachi S-5200 scanning electron microscope. Raman spectroscopy was performed with a Horiba Jobin Yvon spectrometer. X-ray diffraction was performed on a Philips X'Pert Pro Multipurpose X-ray diffractometer with cobalt radiation.

3. Results and discussion

As we have reported before [16], the PILP patches formed at the air/water interface can form a single layer of tabular polygonal calcite or aragonite crystals which grow out of an amorphous film-like layer. However, as the surrounding amorphous film tends to dissolve, the mineral layer breaks down into a loose collection of crystals without structural cohesion. Different from previous studies [16], a novel procedure was used here to produce a highly uniform, continuous PILP layer underneath the block copolymer monolayer, termed "delayed crystallization method", in which an aqueous $NaHCO_3$ solution is injected into the subphase 16 h after the block copolymer had been spread on the subphase. We found this delay period crucial to equilibrate interactions between the monolayer and subphase electrolyte species, as depicted in Fig. 1a. After injection of $NaHCO_3$ solution, the PILP droplets were formed first at the air/water interface due to CO_2 evaporation, then the formed droplets became stuck to the PAA block of the block copolymer monolayer which finally leads to formation of a continuous PILP layer underneath the monolayer. A single PILP/block-copolymer layer can be transferred onto solid substrates, either by approaching the air/water interface from the air side or from the subphase, and then lifting it off horizontally. This leads to a supported thin film with either the block copolymer monolayer or the PILP layer being exposed on top, as shown in Fig. 1b. Subsequent Layer-by-Layer film transfer finally leads to a multilayered thin film which consists of alternating lamellae of organic and PILP monolayers. The PILP droplets adsorb to the monolayer and coalesce to form a smooth and continuous film which rapidly solidifies into a layer consisting of amorphous calcium carbonate (ACC). This ACC layer can then be further transformed into tabular $CaCO_3$ crystals through annealing, i.e. heat treatment. The PILP-to-crystal transformation leads to a multilayered $CaCO_3$/block copolymer composite structure, which bears a striking morphological similarity to nacre (shown in Fig. 1d).

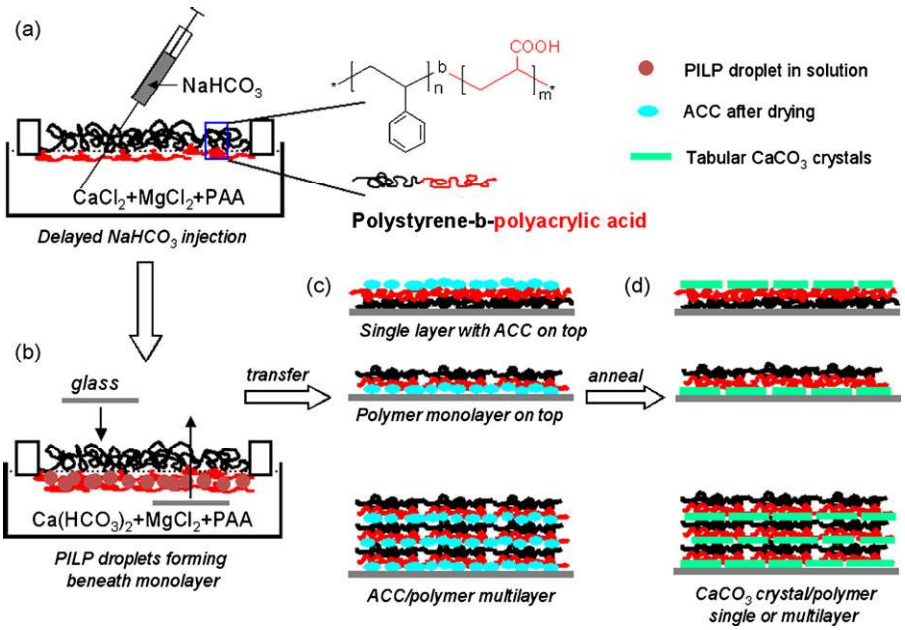

Fig. 1. Schematic illustration of the strategy towards nacre-type multilayer fabrication. (a) Concentrated aq. $NaHCO_3$ solution was injected into the subphase after equilibrating the PS-*b*-PAA block copolymer monolayer for 16 h. (b) Formation of a continuous PILP layer underneath the monolayer. (c) Single or multilayer transfer of composite thin films by approaching the air–water interface with substrate either from air or through the subphase, leading to coatings with either $CaCO_3$ or a block copolymer monolayer on top. (d) Shape preserving pseudomorphic ACC-to-crystal transformation leading to nacre-type multilamellar composite thin films after annealing.

To reveal the morphological characteristics of the PILP layer, which first forms underneath the block copolymer monolayer, the composite film was transferred by approaching the substrate from the air side and lifting it off horizontally. This leads to a thin film on the substrate which exposes the PILP layer on top. Cryo-SEM observations of such films show patches of PILP layers which resemble liquid droplets (Fig. 2a). Occasionally droplets are fused together and form continuous films. We suggest that the PILP droplets accumulate and attach to the monolayer due to the evolution and escape of CO_2 at the air/liquid interface. These PILP droplets could then coalesce and form a continuous film underneath the monolayer, whose thickness increases with time. The film morphology examined with cryo-SEM indicates that the PILP layer was formed by accumulation and coalescence of liquid-like PILP droplets, and that PILP droplet attachment is not homogeneous in different areas underneath the monolayer. On the other hand, SEM images of the same sample after drying in air also show a patchwork morphology, suggesting that the PILP layer could transform into a continuous $CaCO_3$ layer after drying (Fig. 2b). This layer was shown to consist of non-birefringent ACC by polarized optical microscopy. Since this ACC layer originates from a PILP phase, it is anticipated that PAA polyelectrolyte (from the soluble PAA added to subphase as well as PAA segments from the block-copolymer) are firmly attached to the ACC layer. Raman spectra (Fig. 3) of multilayer films transferred onto glass 4 h after $NaHCO_3$ injection show a broad peak centered at 1083 cm^{-1}, which is attributed to amorphous calcium carbonate [21].

To confirm the presence of a composite film with both the organic part and the inorganic PILP layer on the substrate, single layers were transferred onto glass substrates in two different ways, with either the block copolymer monolayer or the PILP side pointing towards the air. AFM topographic images show that the surface of the PILP layer has a roughness of about 4 nm (r.m.s. value calculated by integration over the range of wavelength from 2 μm to 30 nm) and is composed of aggregates of small particles (size: 43 nm) (Fig. 4a). The topographical images of those films with block copolymer monolayers on top reveal different morphologies if compared to those with the PILP surface on top (Fig. 4b). The surface of the copolymer side is rather smooth with a surface roughness of 2 nm (in the wavelength range specified above) and no particles being discernible. These findings are consistent with our assumption that both the calcium carbonate as well as the block copolymer monolayers are well preserved during and after film transfer onto substrates.

PILP layers within multilamellar composite films transform spontaneously into polycrystalline films. However, such kind of transformation can be accelerated with heating. After annealing

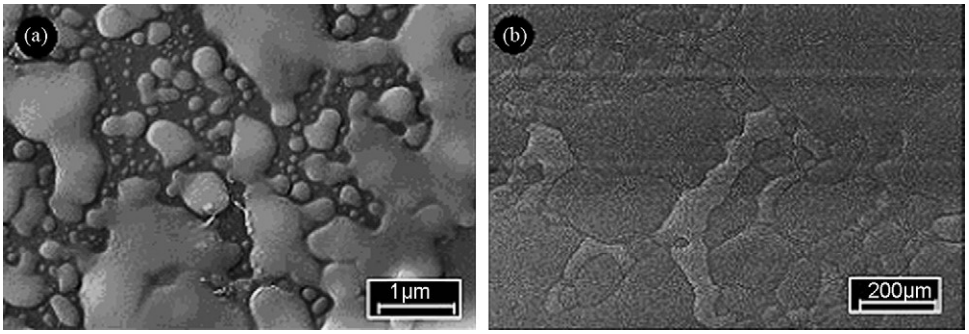

Fig. 2. (a) Cryo-SEM image of a single PILP layer transferred 4 h after injection of $NaHCO_3$ solution into the aqueous subphase. (b) SEM image of the same PILP layer after drying in air.

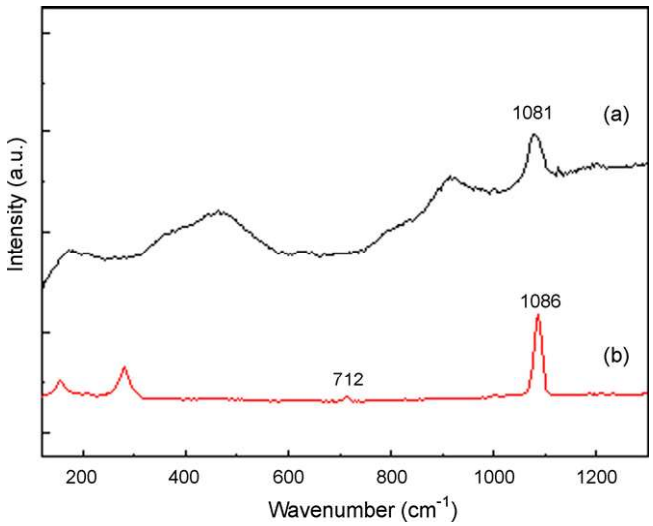

Fig. 3. Raman spectra of the PILP layer before (a) and after (b) annealing.

at 150 °C for 4 h, a continuous monolayer of tabular crystals was observed (Fig. 5a). A time-lapse movie of the transformation process is shown in the supporting information and reveals that the crystal nucleation proceeds in different regions of the PILP phase and then quickly propagates to form a polycrystalline film. The annealed films transferred to the glass substrates (using both methods described earlier) have then been scanned with the AFM, but no changes in the topography can be noticed with respect to the non-annealed film (data not shown). The average surface roughness is about 5 nm and 2 nm, respectively. The characteristic dimensions of primary calcium carbonate particles are well preserved in the polycrystalline films (about 42 nm).

The transformation of amorphous into polycrystalline $CaCO_3$ may proceed through (at least) two fundamentally different phase transition processes [18b], i.e. the solid–solid phase transformation and the dissolution–recrystallization pathway [22,23]. Our time-lapse movie and the unchanged topographies of the $CaCO_3$ layer before and after annealing as revealed by AFM suggest that the transformation from a continuous ACC layer into tabular crystals is

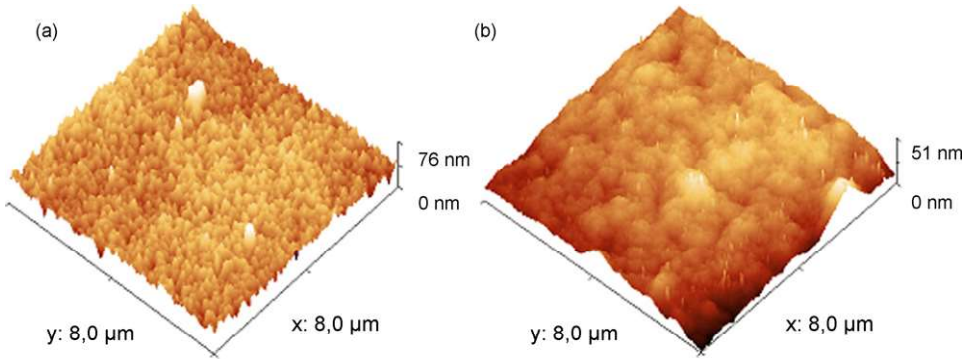

Fig. 4. 3D Tapping mode AFM topographies of the PILP side (a) and PS-*b*-PAA block copolymer monolayer side (b) of a single composite monolayer transferred onto glass before annealing.

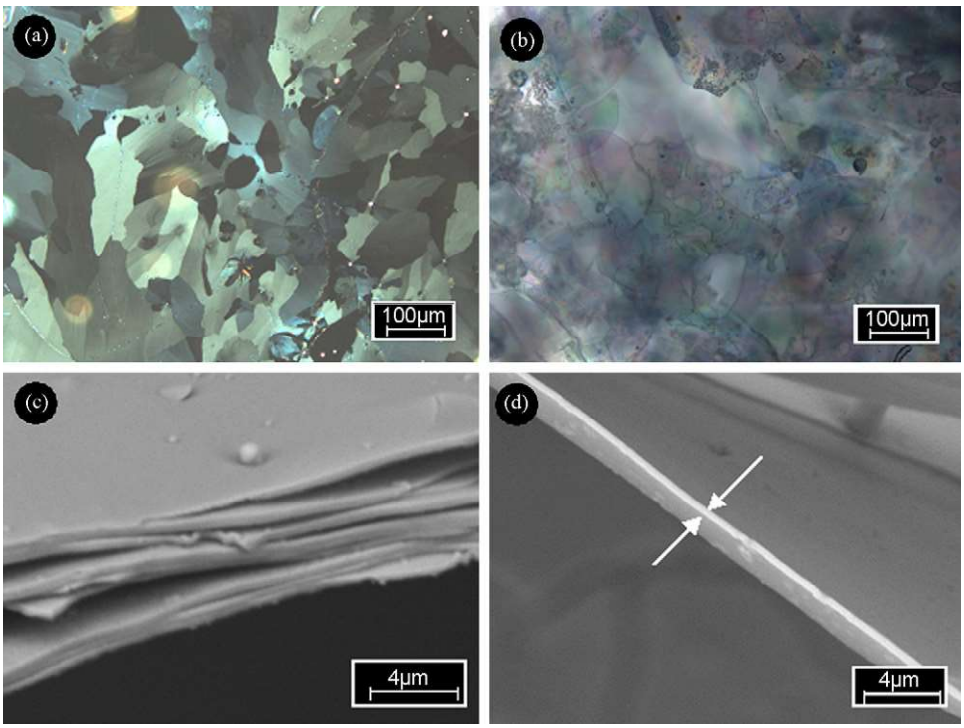

Fig. 5. Optical micrographs of a single layer (a) and a 10-layer (b) of the PILP film after annealing at 150 °C for 4 h. (c) SEM image of a fractured 10-layer film. (d) SEM image of a free-standing calcium carbonate layer which has pealed off from the multilayer. The layer shows a thickness of about 400 nm.

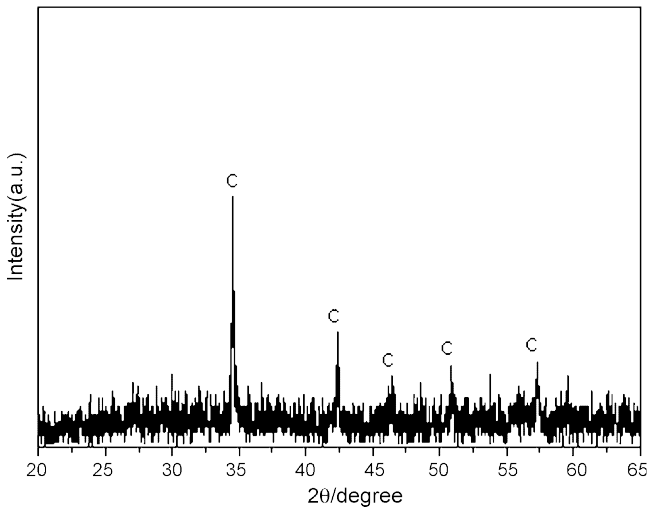

Fig. 6. X-ray diffraction pattern of the multilayer PILP film after annealing. C denotes characteristic Bragg reflections of calcite.

a solid–solid phase transformation process. In addition, the aqueous solvent is removed in the annealing process so that dissolution of ACC is not possible anymore.

In a second step, multiple PILP layers were transferred Layer-by-Layer onto a glass substrate to form a multilayer. After the annealing process the multilayer was investigated with an optical microscope. Fig. 5b shows different interference colors, suggesting that the multilayer thickness and/or the layer composition shows slight alterations in film thickness. Fig. 5c shows a cross-sectional image of an intentionally broken multilayer. Each of the 10 calcium carbonate layers can be identified clearly due to their separation by the organic monolayer. A free-standing single layer was observed (Fig. 5d) as it occasionally pealed off from the multilayer. The average thickness of each single layer is about 400 nm and therewith comparable to the layer thickness of nacre's aragonite tablets. The Raman spectrum of our artificial multilayered films, however, clearly identifies calcite being the major crystalline phase (characteristic peak at 712 cm^{-1}), which is further confirmed by the X-ray powder diffraction pattern shown in Fig. 6.

Simple scratch tests reveal that although our composite thin films bear a layered organic/inorganic hybrid structure, their mechanical strength is much inferior to that of biogenic nacre. We ascribe this marked difference in mechanical performance to the weak interactions of the hydrophobic poly(styrene) moieties with themselves as well as with the polyelectrolyte or crystalline parts of the composite. However, we anticipate that a much stronger cohesion between block-copolymer chains might be achieved by a suitable post-treatment, for instance by cross-linking PS chains via irradiation with hard UV light.

4. Conclusion

In summary, we have shown here a novel strategy to form nacre-type composite multilayers consisting of alternating block copolymer and tabular $CaCO_3$ layers, which form through PILP layer formation at the air/liquid interface. In contrast to our previous study [16], we succeeded to prepare large scale continuous PILP layers underneath the block copolymer monolayer. It was further demonstrated that such block copolymer/PILP composite films could be used to build up organic–inorganic hybrid multilayers through Layer-by-Layer deposition onto solid substrates. By drying in air, the PILP layer on the solid substrate transforms into a continuous layer of ACC, which can be further transformed into tabular calcite crystals by annealing. The characteristic multilamellar architecture of the composite films is preserved through all transformation steps. Our results shown here thus provide a novel approach to mimic and reproduce characteristic morphological features of nacre. As an environmentally benign material, thin films of artificial nacre may have potential applications in anticorrosion coatings, as well as in building architecture or decorative materials. From a more technological point of view, we have shown here one possibility to employ a PILP as a building material for multilamellar composite thin film architectures which as yet have failed to form by alternative production strategies, e.g. epitaxial deposition routes. Provided that further improvement of the mechanical strength could be achieved by tailoring the block-copolymer structure, this method might be of general utility for other inorganic/organic materials which can be produced via PILP formation. Detailed investigations on the transformation mechanisms by which polygonal $CaCO_3$ tablets form from a PILP or ACC phase, respectively are currently underway.

Acknowledgements

The authors thank the Deutsche Forschungsgemeinschaft (DFG) International Materials World Network (MWN) for financial support. Thanks also to Z. Wu and E. Kaltenecker for their help with XRD and Raman spectra measurements, respectively.

References

[1] H.A. Lowenstam, S. Weiner, On Biomineralization, Oxford University Press, New York, 1989.
[2] H. Imai, Y. Oaki, Handbook of Biomineralization: Biomimetic and Bioinspired Chemistry, 2007, pp. 89–107.
[3] Y. Oaki, H. Imai, Angew. Chem. 117 (2005) 6729.
[4] (a) C.M. Ortiz, C. Boyce, Science 319 (2008) 1053;
(b) X.Z. Li, H. Xu, R. Wang, Nano Lett. 6 (2006) 2301.
[5] B.L. Smith, T.E. Schäffer, M. Viani, J.B. Thompson, N.A. Frederick, J. Kindt, A. Belcher, G.D. Stucky, D.E. Morse, P.K. Hansma, Nature 399 (1999) 761.
[6] K. Tushtev, M. Murck, G. Grathwohl, Mater. Sci. Eng. C 28 (2008) 1164.
[7] (a) Z. Tang, N.A. Kotov, S. Magonov, B. Ozturk, Nat. Mater. 2 (2003) 413;
(b) L.J. Bonderer, A.R. Studart, L.J. Gauckler, Science 319 (2008) 1069;
(c) P. Podsiadlo, S. Paternel, J.-M. Rouillard, Z. Zhang, J. Lee, J.-W. Lee, E. Gulari, N.A. Kotov, Langmuir 21 (2005) 11915;
(d) P. Podsiadlo, M. Michel, J. Lee, E.N.W. Verploegen, S. Kam, V. Ball, J. Lee, Y. Qi, A.J. Hart, P.T. Hammond, N.A. Kotov, Nano Lett. 8 (2008) 1762;
(e) Z. Burghard, A. Tucic, L.P.H. Jeurgens, R.C. Hoffmann, J. Bill, F. Aldinger, Adv. Mater. 19 (2007) 970;
(f) F. Bennadji-Gridi, A. Smith, J.P. Bonnet, Mater. Sci. Eng. B 130 (2006) 132.
[8] (a) H. Wei, N. Ma, F. Shi, Z. Wang, X. Zhang, Chem. Mater. 19 (2007) 1974;
(b) T. Kato, T. Suzuki, T. Irie, Chem. Lett. 29 (2000) 186.
[9] N. Gehrke, N. Nassif, N. Pinna, M. Antonietti, H.S. Gupta, H. Cölfen, Chem. Mater. 17 (2005) 6514.
[10] I.M. Weiss, N. Tuross, L. Addadi, S. Weiner, J. Exp. Zool. 293 (2002) 478.
[11] S. Weiner, I. Sagi, L. Addadi, Science 309 (2005) 1027.
[12] L. Addadi, D. Joester, F. Nudelman, S. Weiner, Chem. Eur. J. 12 (2006) 980.
[13] N. Nassif, N. Pinna, N. Gehrke, M. Antonietti, C. Jager, H. Colfen, Proc. Natl. Acad. Sci. U.S.A. 102 (2005) 12653.
[14] E. DiMasi, V.M. Patel, M. Sivakumar, M.J. Olszta, Y.P. Yang, L.B. Gower, Langmuir 18 (2002) 8902.
[15] O. Casse, O. Colombani, K. Kita-Tokarczyk, A.H.E. Muller, W. Meier, A. Taubert, Faraday Discuss. 139 (2008) 179.
[16] F.F. Amos, D.M. Sharbaugh, D.R. Talham, L.B. Gower, M. Fricke, D. Volkmer, Langmuir 23 (2007) 1988.
[17] X. Cheng, L.B. Gower, Biotechnol. Progress. 22 (2006) 141.
[18] (a) L.B. Gower, D.J. Odom, J. Cryst. Growth 210 (2000) 719;
(b) L.B. Gower, Chem. Rev. 108 (2008) 4551;
(c) J. Dai, E.P. Douglas, L.B. Gower, J. Non-Cryst. Solids 354 (2008) 1845.
[19] E.P. Currie, K.A.B. Sieval, G.J. Fleer, M.A.C. Stuart, Langmuir 16 (2000) 8324.
[20] Y.-J. Han, J. Aizenberg, J. Am. Chem. Soc. 125 (2003) 4032.
[21] L. Addadi, S. Raz, S. Weiner, Adv. Mater. 15 (2003) 959.
[22] X. Xu, J.T. Han, D.W. Kim, K. Cho, J. Phys. Chem. B 110 (2006) 2764.
[23] Y. Politi, R.A. Metzler, M. Abrecht, B. Gilbert, F.H. Wilt, I. Sagi, L. Addadi, S. Weiner, P.U.P.A. Gilbert, Proc. Natl. Acad. Sci. U.S.A. 105 (2008) 17362.